NOTES AND CORRESPONDENCE

Westward Intensified and Topographically Modified Planetary Modes

STEFANO PIERINI

Istituto di Meteorologia e Oceanografia, Istituto Universitario Navale, Naples, Italy

12 March 1996 and 25 October 1996

ABSTRACT

The process study presented in this note originates from the interest in investigating the existence of barotropic planetary Rossby modes in Mediterranean subbasins that have relatively small length scales and include extensive topographic slopes. First, the flat-bottom case is considered, then the effect of idealized bathymetries is analyzed. In the flat-bottom case an analytical equilibrium solution of the divergent quasigeostrophic equation forced by a periodic wind stress curl in a circular domain is recovered numerically in the framework of a primitive equation model. The initial spinup phase leading to the establishment of the lowest normal mode, the mode in equilibrium with the wind, and the free mode are then considered in a square domain. The equilibrium response to fluctuating winds reveals a westward intensification (absent in the inviscid theory as well as for free oscillations) that, unlike for steady western boundary currents, increases with increasing lateral friction. A dynamical explanation of this anomalous behavior in terms of vorticity balance is proposed. These westward intensified equilibrium solutions can be seen as the oscillating counterpart of the steady western boundary currents.

The effect of idealized bathymetries is then analyzed. The presence of shelf and slope topographies representing larger and larger regions of intense topographic β effect, while leaving the forced response westward intensified, leads to a progressive shift to lower frequencies of the ground state because of the reduced effective length scale of the basin. Such shift is also accompanied by a remarkable reduction of the amplitude at resonance. For large topographic gradients covering more than 90% of the total basin area (a typical situation for the central Ionian and the Tyrrhenian Seas), the existence of planetary modes and even any sign of westward propagation is prevented by the overwhelming action of the topographic steering. This property, and that for flat-bottom or for less extensive topographies planetary resonances do occur, suggests that the choice of Mediterranean topographies in circulation models should not contain regions of unrealistic flat-bottom, otherwise spurious Rossby resonances could contaminate the model response.

1. Introduction

The Mediterranean Sea dynamics has been, in recent years, the subject of an intense experimental and modeling research activity (e.g., Millot 1987; Robinson et al. 1991; Heburn 1994; Malanotte-Rizzoli and Bergamasco 1991; Beckers 1991; Herbaut et al. 1996; Roussenov et al. 1995; Zavatarelli and Mellor 1995; Pinardi et al. 1997; Pierini and Simioli 1997). Although the basic physical processes involved in the air–sea interaction, the deep-water formation, the thermohaline circulation, the internal mesoscale dynamics, etc., are essentially the same as for large oceans, the resulting circulation shows features such as a strong seasonality and reversal of currents and a large interannual variability that are peculiar to this ''small ocean.'' Analogously, it is interesting to inquire whether the Rossby dynamics, which has proved so important in accounting for the variability of large oceans, plays a relevant role also in the Mediterranean Sea, that is, in a situation in which the scales and the topography are so specific. In this respect, in this note a numerical process study is presented concerning the possibility of the existence of planetary Rossby modes in the Mediterranean Sea. In order to explain why this problem arises let us briefly review the basic general concepts and implications related to the Rossby dynamics.

The barotropic Rossby waves and modes contribute to determine the subinertial oceanic response to large-scale winds. Their existence derives from the conservation of potential vorticity attached to any fluid column and can be of planetary or topographic origin, and in the form of waves (infinite ocean) or normal modes (limited ocean). For planetary Rossby waves (PRWs) the restoring force is provided by the variation of the Coriolis force with latitude, while topographic Rossby waves (TRWs) are trapped over topographic features and derive from a predominantly topographic β effect; finally, an intermediate case (which one might term to-

Corresponding author address: Dr. Stefano Pierini, Istituto Universitario Navale, Istituto di Meteorologia e Oceanografia, C. So Umberto I, 174, I-80138 Naples, Italy.
E-mail: pierini@nava1.uninav.it

pographically modified PRWs) is that of PRWs, which are locally modified by topographic variations but retain their planetary nature. On the other hand, the continuous spectrum associated to free or forced waves traveling in the open ocean is complemented by a discrete spectrum associated to planetary or topographic Rossby normal modes (PRMs, TRMs). They are excited resonantly and owe their existence to the presence of coasts or strong topographic gradients that, through reflections, select specific wavelengths, the dispersion relation determining the corresponding eigenfrequencies (e.g., Le Blond and Mysak 1978; Pedlosky 1987).

The Rossby wave dynamics has proved successful in describing important features of oceanic currents (particularly in the North Atlantic and Pacific Oceans) such as, for instance, the westward intensification of boundary currents (Pedlosky 1965a), the response to large-scale fluctuating winds (e.g., Pedlosky 1965b; Leetma 1978; Harrison 1979; Willebrand et al. 1980; Frankignoul and Müller 1979), boundary current radiation, and, more in general, the intrinsic forcing of midocean eddies (e.g., Pedlosky 1977; Malanotte-Rizzoli et al. 1987; Miller et al. 1987; Malanotte-Rizzoli and Young 1988), etc. In theoretical studies PRMs often arise because the limited extent of even a large ocean, such as the Atlantic, can lead to the excitation of normal modes. Willebrand et al. (1980) computed the ratio $r = T_{\text{diss}}/T_{\text{prop}}$ between the characteristic timescale of dissipation and the time it takes a Rossby wave to propagate westward across the basin and found that for the Atlantic Ocean $r > 1$ (and so basin modes can be established) for the 4–5 lowest modes, corresponding to periods ranging from 10 to 15 days. However, in the Atlantic PRMs have never been unambiguously observed, while in the Pacific Luther (1982) showed persuasive evidence of a PRM of 4–6 days with an energy *e*-folding time of less than three days.

Now, what can be said about the existence of PRMs in the Mediterranean Sea? In the framework of a flat-bottom analytical process study Pierini (1990) noticed that for the typical dimensions and mean depths of Mediterranean subbasins, the lowest Rossby eigenperiod T_0 can be of the order of 1 month or more, compared to just 10 days for the Atlantic. Also the spectral separation between the first few modes should be larger in the Mediterranean than in the Atlantic (where the modes are clustered about T_0), so that in Mediterranean subbasins one could in principle expect the lowest PRMs to manifest themselves in the form of recognizable westward traveling patterns, corresponding to well-separated peaks in the power spectrum. Another important difference between the two cases is that, while in the Atlantic PRMs determine the high-frequency response to the wind [$T \leq O$ (10 days)], in the Mediterranean they would intervene to affect the seasonal variability.

However, these conjectures are based on computations in which topographic variations are totally neglected, being just taken into account to compute an average depth. Is this appropriate in the case of the Mediterranean Sea? Consider the following numerical results: westward propagating features in the Eastern Mediterranean, interpreted as wind-induced PRMs, were obtained in a wind-driven GCM (Pinardi and Navarra 1993) in which the bottom topography was approximated by a plateau at 1100-m depth. However, in the same study and in that by Roussenov et al. (1995), when the topography was satisfactorily resolved, such features appeared greatly attenuated. This suggests that the topography plays a major role in the character of PRMs: again, the Mediterranean Sea differs markedly from large oceans also in relation to this aspect. Indeed, while, for example, in the Atlantic, the effect of topographic features such as the midocean ridge or shelves on the propagation, transmission, and absorption of PRMs was found to be important (e.g., Rhines 1969; Kroll and Niiler 1976; Anderson and Killworth 1977; Barnier 1984a,b; Miller 1986; Wang and Koblinsky 1994; Matano 1995), but not so dramatic to destroy the very existence of PRMs, in the Mediterranean the topographic β effect is large almost everywhere so that one wonders whether PRMs, though modified by the topography, can exist [a different matter is the possibility of existence of TRMs, which can be expected in localized regions of the Mediterranean, as shown by Candela and Lozano (1994) and Pierini (1996), and for which the first clear observational evidence in world oceans has been provided very recently by Miller et al. (1996) in the Iceland–Faeroe ridge].

In this note, an idealized numerical process study is developed aimed at understanding the effect on PRMs of a bottom topography that, like in Mediterranean subbasins, is formed by wide shelf escarpments that can cover a large portion of the domain. This numerical study can be seen as the generalization of the analytical study by Pierini (1990) to the case in which bottom and lateral friction and topographic variations are present. Therefore, in section 2, in order to match the present model with the analytical one, the analytical solution of the quasigeostrophic equation describing forced Rossby modes in a circular domain with flat bottom is reproduced numerically by solving an initial value problem for the shallow-water equations with a white wind forcing. Subsequently, a numerical experiment is presented in which the initial spinup phase leading to the establishment of the normal mode, the mode in equilibrium with the wind, and the free decaying mode are described. An interesting feature of the forced response is a clear westward intensification, which disappears when the wind is switched off and the mode evolves freely, decaying because of lateral and bottom friction. In section 3 the westward intensification of the equilibrium solution is considered in detail. It is found that the intensification increases with increasing lateral friction coefficient, unlike for a steady western boundary current for which the opposite behavior holds. A dynamical

explanation of this anomalous behavior in terms of vorticity balances is proposed.

In section 4 we then pass to introduce idealized topographies representing larger and larger regions of intense topographic β effect. Their presence, while leaving the forced response westward intensified, leads to a shift toward smaller frequencies of the Rossby eigenmodes (because of smaller and smaller effective regions on which the planetary β effect can act) and amplitudes remarkably reduced at resonance. These results confirm the expected important role played by the topography: The Mediterranean topographic variations are so strong and extensive that, for instance, in the Tyrrhenian or in the central Ionian Basin, PRMs can hardly exist. On the other hand, in subbasins where regions of very small topographic gradients are present (e.g., the Provençal Basin west of Sardinia or the southwestern Ionian Sea) the existence of planetary resonances cannot, in principle, be ruled out. Of course, TRMs may be expected to determine locally the relatively high-frequency (few days) wind-driven response. Finally, the same results also indicate that the topography needs to be well resolved in circulation models of the Mediterranean, otherwise spurious PRMs could affect the dynamics produced by the model.

2. Wind-driven response and free oscillations: Flat bottom

In a process study aimed at determining the response to a fluctuating wind forcing in a closed domain, Pierini (1990) considered the linearized, forced, divergent quasigeostrophic equation

$$\frac{\partial}{\partial t}\left(\nabla^2\psi - \frac{\psi}{L^2}\right) + \beta\psi_x = F \tag{1a}$$

$$L = \frac{\sqrt{gD}}{f_0}, \quad F(\mathbf{x}, t) = \frac{\mathrm{curl}_z\tau_w}{\rho D}, \tag{1b}$$

where g is the acceleration of gravity, D is the constant water depth, $f = f_0 + \beta y$ is the Coriolis parameter, L is the external Rossby deformation radius, τ_w is the wind stress, ρ is the water density, and $\psi(\mathbf{x}, t)$ is the streamfunction of the flow, from which the velocity $\mathbf{u} = (\psi_y, -\psi_x)$ and the free surface displacement $\eta = -(f_0/g)\psi$ can be computed. The boundary conditions to be associated to the divergent problem (1a,b) are

$$\psi\big|_{\partial E} = C(t), \quad \frac{\mathrm{d}}{\mathrm{d}t}\oint_{\partial E} \nabla\psi\cdot\mathbf{n}\, \mathrm{d}s = \iint_E F \mathrm{d}^2x, \tag{2}$$

where the first expression [$C(t)$ is an unknown function of time] corresponds to the free-slip boundary conditions and the second one expresses the conservation of mass. For a circular domain E of radius R and for a spatially constant wind stress curl oscillating with frequency Ω, $F(t) = \tilde{F}\exp(-i\Omega t)$, the equilibrium solution of (1), (2) in polar coordinates (r, θ) valid continuously also for frequencies larger than the highest Rossby eigenfrequency reads (Pierini 1990)

$$\eta_\Omega(\mathbf{x}, t) = \frac{i\tilde{F}f_0L^2}{g\Omega}\left[1 - \frac{R}{4\lambda L^2}\frac{\varphi(\Omega, \mathbf{x})}{\Gamma(\Omega)}\right]e^{-i\Omega t}, \tag{3}$$

(the real part of the right-hand side is implied) where

$$\left.\begin{aligned} \varphi(\Omega, \mathbf{x}) &= \sum_{m=0}^{\infty}\frac{2}{a_m}i^m\frac{J_m(kR)}{J_m(\lambda R)}J_m(\lambda r)\cos(m\theta)e^{-ikr\cos\theta} \\ \Gamma(\Omega) &= \sum_{m=0}^{\infty}\frac{J_m^2(kR)}{a_m}\frac{J_m'(\lambda R)}{J_m(\lambda R)} \\ \lambda^2 &= k^2 - L^{-2}, \quad k = \frac{\beta}{2\Omega}, \quad a_m = \begin{cases} 2, & m = 0 \\ 1, & m \geq 1 \end{cases} \end{aligned}\right\}$$

and where J_m are the Bessel functions of the first kind. On the other hand, the homogeneous version of (1), (2) ($F = 0$) admits solutions in the form of PRMs:

$$\eta_n(\mathbf{x}, t) \propto \frac{f_0}{g}\varphi_n(\mathbf{x})e^{-i\bar{\Omega}_n t}, \tag{4}$$

where the eigenfrequencies $\bar{\Omega}_n$ and the (complete and orthogonal set of) eigenfunctions φ_n are given by

$$\Gamma(\bar{\Omega}_n) = 0, \ \varphi_n(\mathbf{x}) = \varphi(\bar{\Omega}_n, \mathbf{x}).$$

Thus, the equilibrium response (3) resonates at the Rossby eigenfrequencies of the system, although solution (3) does not provide the amplitude for $\Omega = \bar{\Omega}_n$ because no limiting mechanisms such as dissipation and nonlinearities are taken into account.

If we now consider a ''white'' forcing,

$$F(t) = \frac{\tilde{F}}{N}\sum_{k=1}^{N}\sin(\Omega_k t), \tag{5}$$

where $\Omega_N = 2\pi/T_{\min}$, $\Omega_1 = 2\pi/T_{\max}$, and $\Omega_k = (k - 1)(\Omega_N - \Omega_1)/(N - 1) + \Omega_1)$, the response will be given by

$$\eta(\mathbf{x}, t) = \frac{1}{N}\sum_{k=1}^{N}\eta_{\Omega_k}(\mathbf{x}, t), \tag{6}$$

where each $\eta_{\Omega_k}(\mathbf{x}, t)$ is provided by (3). We want to compare (6) with the corresponding numerical solution in the framework of the linear shallow-water dynamics

$$\left.\begin{aligned} \mathbf{u}_t + f\,\mathbf{k}\times\mathbf{u} &= -g\nabla\eta + \frac{(\tau_w - \tau_b)}{\rho H} + A_H\nabla^2\mathbf{u} \\ \eta_t + \nabla[(D - d)\mathbf{u}] &= 0 \end{aligned}\right\}, \tag{7}$$

where $\mathbf{k} = (0, 0, 1)$, A_H is the lateral eddy viscosity coefficient, $\tau_b = \rho C_{Db}|\mathbf{u}|\mathbf{u}$ is the bottom stress, and $d(\mathbf{x})$ is the bottom topography. The geostrophic velocities implied by (1a) are not directly comparable to the shallow-water velocities in (7) because the latter include also the ageostrophic Ekman transport; moreover (7)

includes frictional effects that are absent in (1a). However, the comparison between the two sea surface displacements (away from the boundary layers) is justified because η in (7) drives the pressure-driven velocities that, in the quasigeostrophic limit, correspond to those of (1a). In this framework the forcing for (7) corresponding to (5) is given by

$$\tau_w(\mathbf{x}, t) = \left(\chi\frac{y}{R}, 0\right)\frac{1}{N}\sum_{k=1}^{N}\sin(\Omega_k t), \tag{8}$$

where $\chi = R\rho D\tilde{F}$ and, in analogy with the analytical solution, the origin of the axis is taken in the center of the square. The initial value problem with no-slip boundary conditions and vanishing initial conditions for problem (7) forced by (8), in a square domain of length 2R, is solved numerically by means of a finite-difference method (Pierini 1996). The parameter values common to the analytical quasigeostrophic and numerical shallow-water solutions are $f_0 = 0.9 \times 10^{-4}$ rad s^{-1}, $\beta = 1.82 \times 10^{-11}$ rad m^{-1} s^{-1}, $T_{\min} = 10$ days, $T_{\max} = 400$ days, and $N = 500$; the constant depth $D = 2000$ m ($d = 0$) and the radius $R = 500$ km are chosen as representative of typical Mediterranean subbasins. In (7) $A_H = 500$ m^2 s^{-1} and $C_{Db} = 0.002$ and the resolution is $\Delta x = \Delta y = 50$ km and $\Delta t = 30$ s. The forcing is $\chi = 1$ dyn cm^{-2} in (8), corresponding to a curl$\tilde{F} = (2 \times 10^{-8}$ dyn cm$^{-3})/(\rho D)$ in (5) representing a typical order of magnitude for the wind stress curl in the Mediterranean. The importance of the nonlinear terms $(\mathbf{u}\cdot\nabla)\mathbf{u}$ in the momentum equations and $\nabla(\eta\mathbf{u})$ in the continuity equation were tested by including them in several runs. Their effect was found to be totally negligible, and this for wind forcings of realistic amplitudes. In other words no rectified circulation is to be expected in the following numerical experiments.

In Fig. 1a the spectrum of forcing (5) is reported, while Fig. 1b shows the spectra of the response given by (6) and by the numerical solution of (7) referring to the central point of the domain. The analytical (inviscid) and numerical (viscous) solutions are in good agreement near the primary resonance. They both give a resonance at about $T = 38$ days, corresponding to the lowest PRM; the amplitude of the analytical inviscid solution is obviously larger than the numerical viscous one, but not so much near the resonant frequency. Closer to resonance the inviscid solution diverges, while the viscous response has a finite value. The second mode, corresponding to $T = 70$ days (not shown but corresponding to the out-of-scale resonance at low frequency in the analytical spectrum) is not resolved by the numerical model because of the low resolution used, which has also implied the use of a square domain instead of a circle, as for the analytical solution. Nonetheless the numerical eigenfrequency in the square has evidently not been appreciably shifted with respect to the analytical eigenfrequency in the circle, because the zonal extent of the two domains is the same at $y = R$, so the

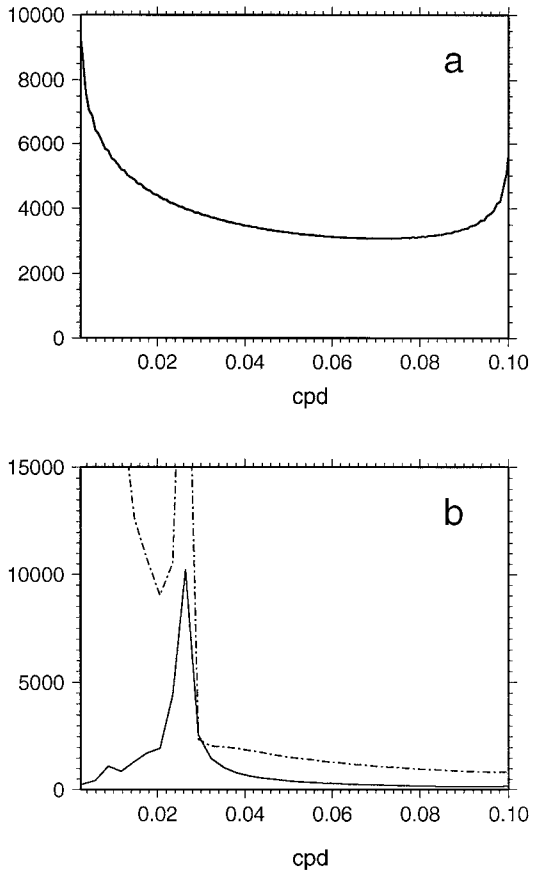

FIG. 1. (a) Spectrum of the forcing function (5). (b) Spectrum of the corresponding sea surface elevation in the middle of the basin given by the analytical solution (6) (dashed line) and by the numerical solution of (7) forced by (8) (solid line).

Rossby mode properties are not expected to differ notably.

In order to analyze the structure of the lowest PRM, model (7) is forced by

$$\tau_w(\mathbf{x}, t) = \left(\chi\frac{y}{R}, 0\right)q(t)\sin(\Omega t), \quad q(t) = \begin{cases}1, & t \le 4T\\ 0, & t > 4T,\end{cases} \tag{9}$$

where $\Omega = 2\pi/\mathrm{T}$ ($\mathrm{T} = 37.88$ days) is chosen equal to the eigenfrequency under consideration. The response to (9) shows (Fig. 2) the initial spinup phase leading to the establishment of the normal mode, the mode in equilibrium with the wind and, for $t > 4T$, the free mode, eventually decaying because of dissipative effects. The spinup is completed in about two cycles: for $t < T/2$ the negative vorticity input induces an anticyclonic circulation moving westward (Fig. 2b) accompanied by the birth of a cyclonic gyre at the eastern side of the basin for $T/2 < t < T$. The reflection of the Rossby wave at the western boundary then leads to the asymptotic oscillating circulation already after the second cycle. For $2T < t < 4T$ (i.e., until the wind is switched

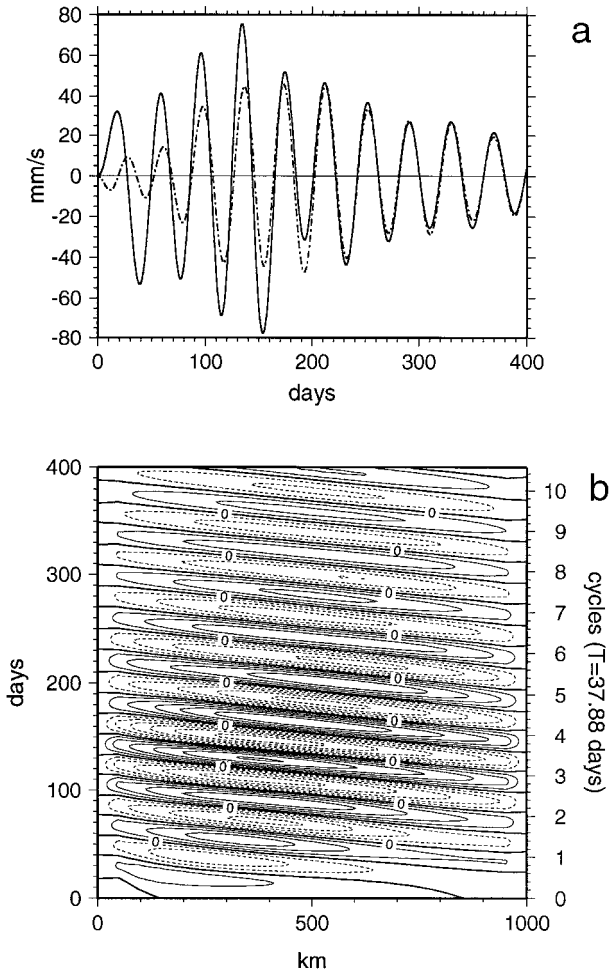

FIG. 2. Numerical solution of (7) forced by (9) with $T = 37.88$ d at $y = 0$ (equidistant from the northern and southern boundaries). (a) Meridional velocity taken 100 km east of the western boundary (solid line) and 100 km west of the eastern boundary (dashed line). (b) Sea surface elevation as a function of time. The inclination of the isolines indicates westward propagation.

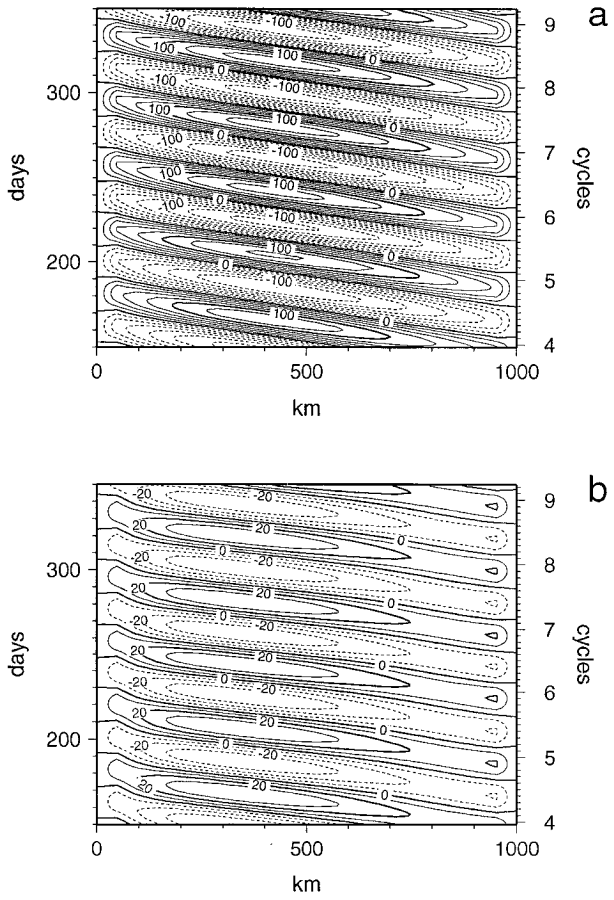

FIG. 3. Numerical solution of (7) forced by (9) with $T = 37.88$ d and $q = 1$ at $y = 0$. Sea surface elevation corresponding to the choice $A_H = 500$ m^2 s^{-1} (a) and $A_H = 10\,000$ m^2 s^{-1} (b).

off) one can observe the equilibrium solution, which appears to be westward intensified, as results clearly show both from the x–t diagram (Fig. 2b) and from the comparison between the western and eastern meridional velocities (Fig. 2a, see the next section for more details). For larger times the basin oscillation evolves toward a free, decaying PRM for which the westward intensification disappears (see, for instance, the field for $t > 6T$). In conclusion we have found that, while the amplitude as a function of frequency of the numerical (viscous) response agrees fairly well near primary resonance with the analytical (inviscid) one, the structure of the viscous forced solution yields westward intensification. On the other hand, the presence of dissipative effects leaves virtually unaltered the frequency and structure of the inviscid free normal modes, apart from the amplitude decay.

3. The westward intensification of wind-driven Rossby oscillations

The westward intensification of the equilibrium forced solution as results from Fig. 2 is an interesting feature that will be considered in detail in this section. First, it is worth noticing that, while in the theory of steady western boundary currents, the intensification is usually denoted by means of the width of the western boundary layer l, heretofore we will refer to a generic westward intensification of Rossby oscillations (whose quantitative definition is beyond the scope of this note). In fact, in the periodic case the intensification does not manifest itself necessarily as a narrow, time-dependent western boundary layer (in which case a trivial generalization of l would be available), but rather as westward propagating, nearly meridional current patterns whose amplitudes are larger to the west than to the east (e.g., see Fig. 2a). It is therefore in this sense that we speak of intensification of the periodic forced response. Let us also stress again that such westward intensification is present in the equilibrium forced solution only, the free modes being completely symmetrical; moreover, it is present not only at resonance but (as it results from

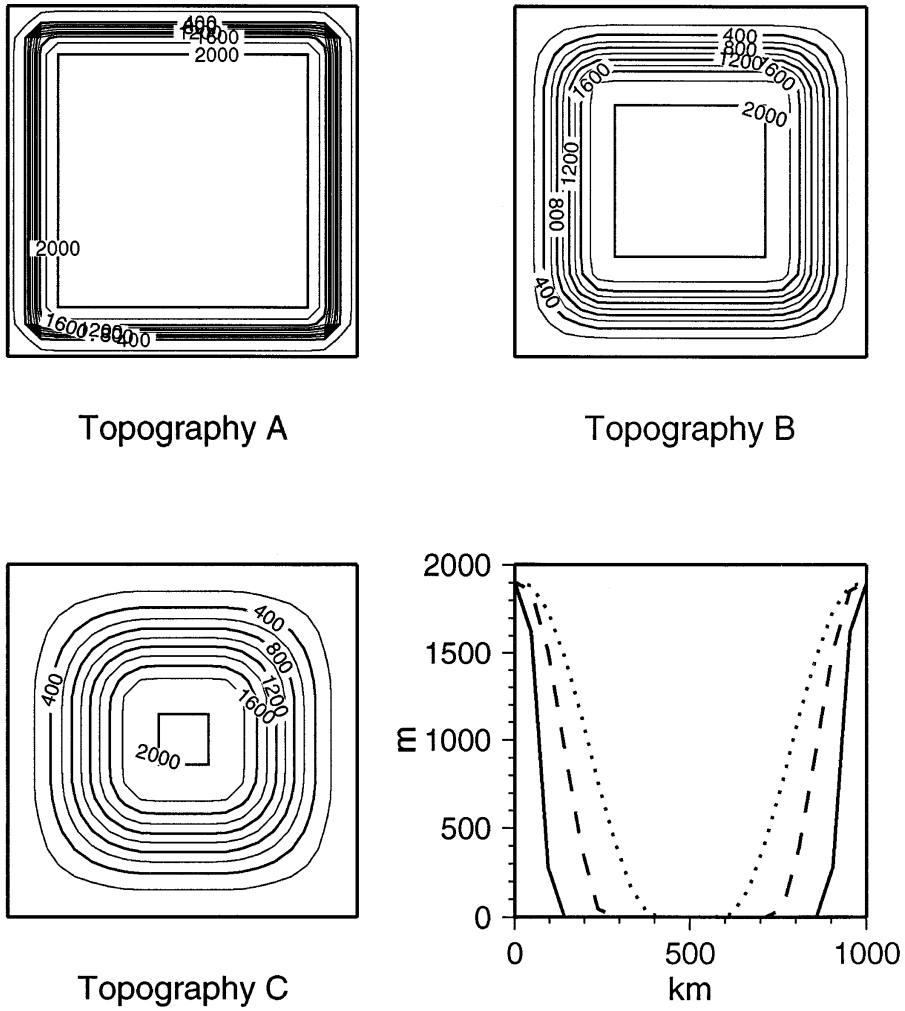

FIG. 4. Bottom depths used in the variable topography runs. In the graph, sections of $d(\mathbf{x})$ at $y = 0$ are given for topography A (solid line), B (dashed line), and C (dotted line).

numerical experiments not shown) also far from resonance, where naturally the response is much weaker. The east–west asymmetry of the forced response cannot be explained by an inviscid wind-driven theory (Pierini 1990) nor by a theory that includes linear bottom friction, at least at first order in the expansion in powers of a damping parameter (Pedlosky 1965b). Indeed, in both cases the forced solution is shown to be symmetrical [e.g., see (3) for the inviscid case], apart from a preferred direction of the phase speed, and corresponds to the normal mode at resonance and resembles the closest normal mode away from resonance.

The only effects missing in the analytical theories quoted above that are included in model (7) are a quadratic bottom friction and the horizontal eddy viscosity; therefore the westward intensification of the periodic forced response here obtained is presumably produced by at least one of these two effects. However, the former is found to be completely irrelevant as far as the intensification is concerned because (as it results from numerical experiments not shown) large variations of C_{Db} leave it unaltered, apart from a sensible variation of the amplitude. As a consequence the eddy viscosity should be responsible for the intensification. This is confirmed by the numerical experiments reported in Fig. 3. In Fig. 3a the forced response at resonance [forced by (9) with $q = 1$ at any time] is shown for the choice $A_H = 500$ m^2 s^{-1} (the same as in the run of Fig. 2), while in Fig. 3b the solution for $A_H = 10\ 000$ m^2 s^{-1} is reported. Apart from the amplitude, which is obviously smaller in the second case, the westward intensification appears more intense in the more viscous case.

It should be noticed that, while the westward intensification of the periodic response increases with increasing A_H (at least within the range of values of A_H considered here), the opposite holds in the case of a steady western boundary current for which a measure of the intensification, for example, the inverse of the width of the Munk layer, decreases with increasing A_H as (e.g., Pedlosky 1987)

$$l^{-1} = \left(\frac{\beta}{A_H}\right)^{1/3}.$$

This anomalous behavior can be explained as follows. Let us first consider a steady western boundary current. This is an intrinsically viscous flow, which derives its steady character by the very existence of lateral friction: its vorticity input on the west side balances the loss (or gain, depending on the sign of the wind stress curl) of relative vorticity due to the wind and the induction by planetary vorticity, while the Sverdrup balance on the east side holds, being virtually unaffected by viscosity. Thus, a larger value of A_H provides the same vorticity input through a weaker western shear, corresponding to a weaker westward intensification. Quite different is the situation of an inviscid Rossby oscillation in equilibrium with the wind. In this case the departure from the Sverdrup balance is everywhere compensated instantaneously by the inertial term giving the rate of change of relative vorticity [the first term in the lhs of (1a)] instead of viscosity. Here, however, no asymmetry is introduced in the flow structure, as stressed above.

If, on the other hand, lateral friction is present [given by a term $A_H\nabla^4\psi$ to be added to the rhs of (1a)], this balance is modified in such a way that the concurrent action of wind, β effect, and viscosity produces a westward intensification in a manner analogous to that of a western boundary current. However, since in the limit $A_H = 0$ the solution is symmetrical, the intensification must increase with increasing A_H, at least for moderate values of lateral friction. In summary, in the highly idealized linear model made of a spatially constant wind stress curl with a mean and a fluctuating part given by a sum of Fourier components, in the limit $A_H \to 0$ the westward intensification is concentrated in the steady boundary current, whereas for increasing values of A_H it manifests itself also in the fluctuating component while it is weaker and weaker in the steady part of the flow.

The westward intensification of forced Rossby oscillations was already noticed in the context of long-period tidal models (Wunsch 1967; Carton 1983; Miller et al. 1993), but no anomalous behavior of the intensification was observed when eddy viscosity was considered (this is not surprising in view of the difference between the wind-driven and the long-period tidal problems). Therefore, the behavior of the intensification described above appears to be peculiar to the present wind-driven model.

4. Wind-driven response and free oscillations: Variable topography

In sections 2 and 3 the analytical inviscid and the numerical viscous theories of wind-driven fluctuations in a closed domain with flat bottom have been analyzed. We are now ready to pass to the more realistic case in which, in the framework of the numerical shallow-water model (7), a variable bottom topography $d(\mathbf{x})$ is introduced. It is chosen as a continental shelf for which the shallow water along the coasts (100 m) is connected to deep water (2000 m) through a sinusoidal slope (Fig. 4). Three cases are considered: topography A is a narrow shelf for which the central flat-bottom deep water region covers about 80% of the domain, topography B represents an intermediate case; while for topography C the area of the deep water region is less than 5% of the total. This last case represents very schematically situations like that of the Tyrrhenian Sea or the central Ionian Basin, while milder topographies like those of cases A and B resemble more the Provençal Basin west of Sardinia or the southwestern Ionian Sea, where regions of small topographic gradients are present.

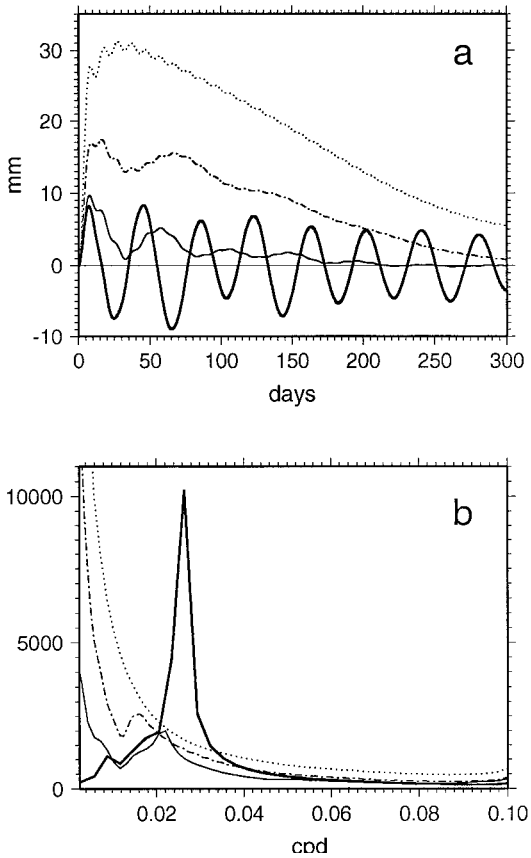

FIG. 5. Numerical solution of (7) forced by (8). (a) Sea surface elevation in the middle of the basin in the flat-bottom case (thick solid line) and for topography A (solid line), B (dashed line), and C (dotted line). (b) Corresponding spectra.

Figure 5 shows the response to forcing (8) in the middle of the basin (Fig. 5a) and the corresponding spectra (Fig. 5b) for the flat-bottom case (thick solid line, equal to the solid line of Fig. 1b) and for topography A (solid line), B (dashed line), and C (dotted line). Two features are immediately apparent. First, the flat-bottom resonance at $T = 37.88$ d shifts to lower frequencies for more and more extensive topographies ($T = 45.45$ d for topography A and $T = 62.5$ d for to-

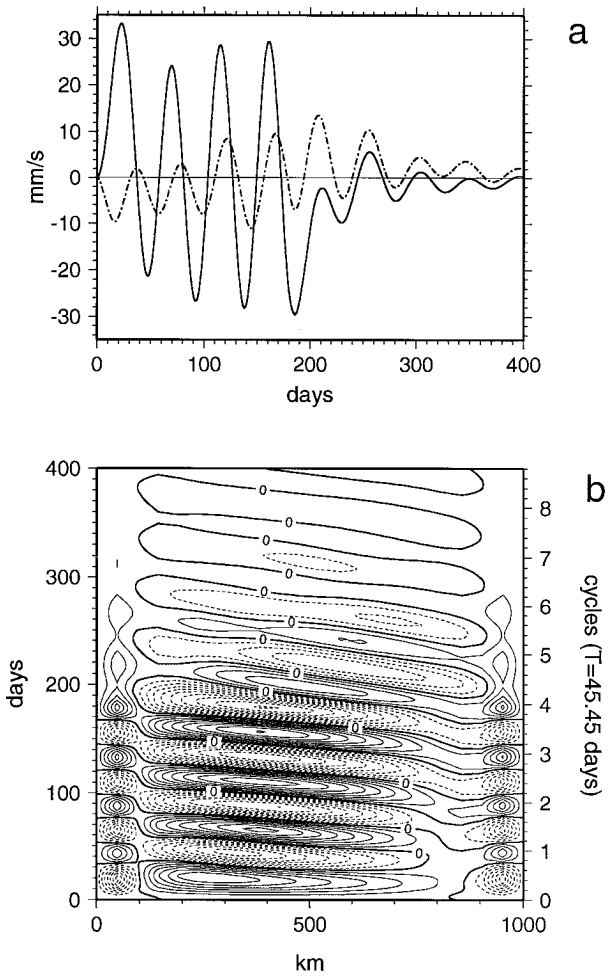

FIG. 6. Numerical solution of (7) forced by (9) for topography A with $T = 45.45$ d at $y = 0$ (equidistant from the northern and southern boundaries). (a) Meridional velocity taken 150 km east of the western boundary (solid line) and 150 km west of the eastern boundary (dashed line). (b) Sea surface elevation as a function of time. The inclination of the isolines indicates westward propagation.

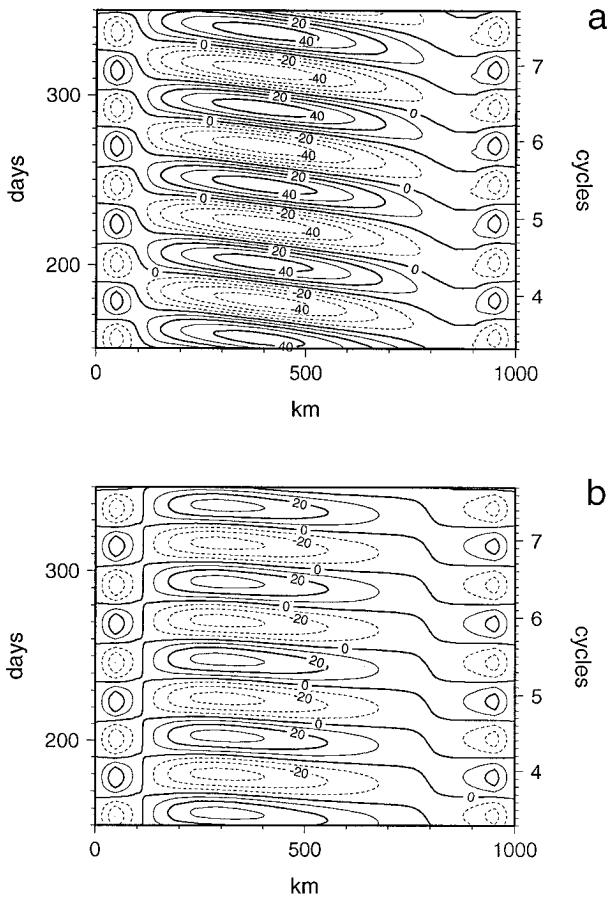

FIG. 7. Numerical solution of (7) forced by (9) for topography A with $T = 45.45$ d and $q = 1$ at $y = 0$. Sea surface elevation corresponding to the choice (a) $A_H = 500$ m^2 s^{-1} and (b) $A_H = 10\,000$ m^2 s^{-1}.

pography B, while topography C does not yield any resonant peak). Second, the amplitude of the resonance decreases markedly when the topography is present. The shift to lower frequencies can be explained by considering that the large topographic β effect associated with the coastal shelf and slope regions acts as an equivalent lateral boundary as far as the reflection of Rossby waves is concerned, according to results concerning the reflection properties of topographic barriers (e.g., Barnier 1984a; Wang and Koblinsky 1994; Matano 1995). The consequent reduction of the effective area over which the mode adjusts implies a reduction of the resonant frequency. At the same time, since the ''topographic'' boundaries also transmit some energy to the shallow coastal waters, the reflected energy giving rise to the normal mode will be smaller than that of the flat-bottom case, so that the amplitude of the modes will be smaller as a result.

In Fig. 6 the same numerical experiment of Fig. 2 is reported in the case of topography A. The westward propagation associated with the PRM is limited to the flat-bottom area, in agreement with the discussion above, while over the shelves the sea level cooscillates with the forcing (see also Fig. 10 below). The westward intensification during the forced phase is present also in this case with variable topography and, again, it disappears in the unforced evolution, during which the dissipative effects act more efficiently than in the flat-bottom case. Comparing Fig. 6 with Fig. 2, one can notice that the intensification of the forced lowest PRM has a more pronounced character for topography A than in the flat-bottom case. Figures 7a and 8a show the response at resonance for topographies A and B with $A_H = 500$ m^2 s^{-1} and $q = 1$ at any time, and when compared with the response at resonance for flat-bottom (Fig. 3a) they show the general tendency for an increased intensification for more extensive topographies, the effective western boundary being approximately given in each case by the line of maximum depth, east of which the topographic gradient vanishes.

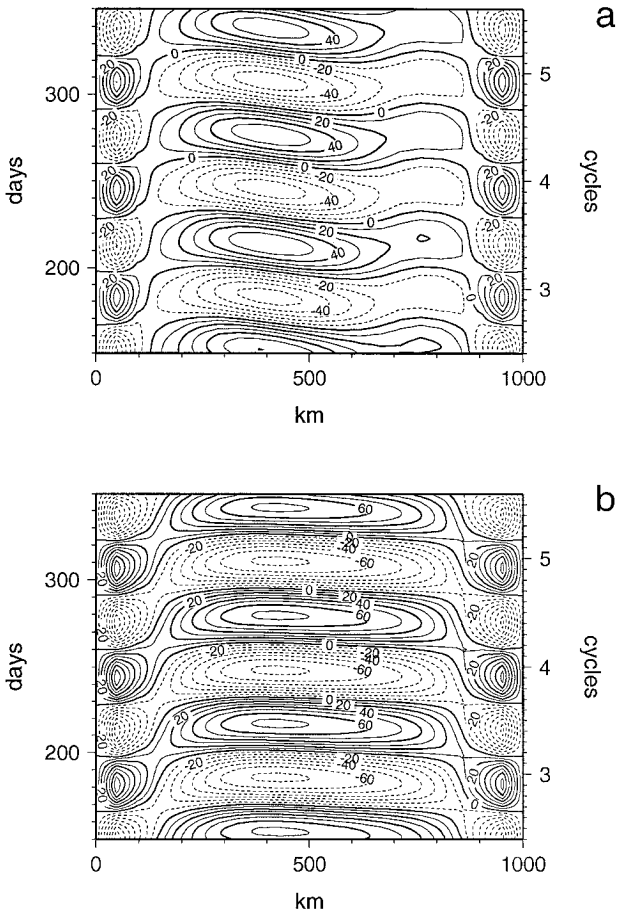

FIG. 8. Numerical solution of (7) forced by (9) for topography B with $T = 62.5$ d and $q = 1$ at $y = 0$. Sea surface elevation corresponding to the choice (a) $A_H = 500$ m^2 s^{-1} and (b) $A_H = 10\,000$ m^2 s^{-1}.

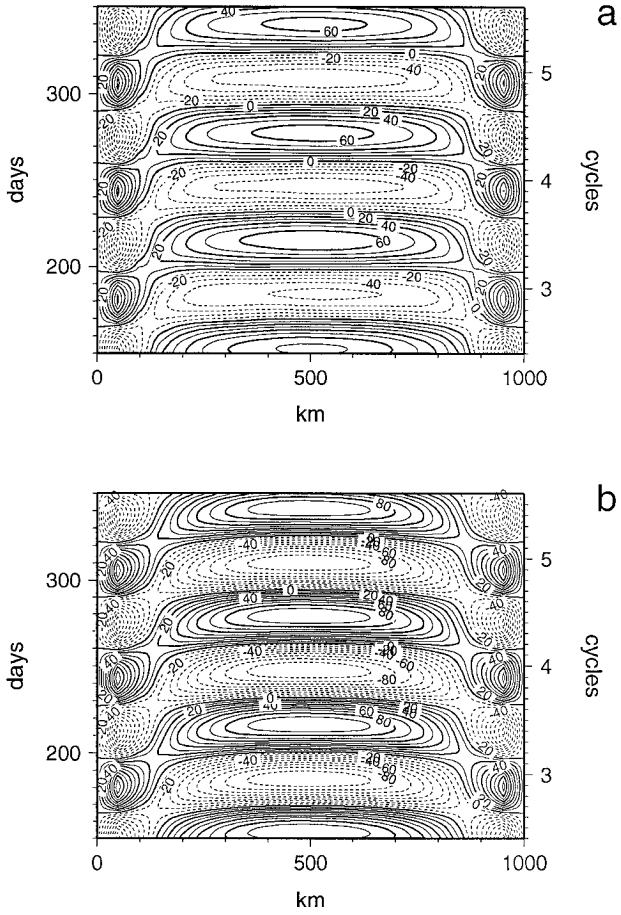

FIG. 9. Numerical solution of (7) forced by (9) for topography C with $T = 62.5$ d and $q = 1$ at $y = 0$. Sea surface elevation corresponding to the choice (a) $A_H = 500$ m^2 s^{-1} and (b) $A_H = 10\,000$ m^2 s^{-1}.

The effect of increasing the lateral friction on the intensification is shown in Figs. 7 and 8 for topographies A and B, respectively, where the cases $A_H = 500$–$10\,000$ m^2 s^{-1} are compared in the continuously forced run. Also in this case the intensification increases as friction increases like in the flat-bottom case, but furthermore another effect is revealed that was present, though less evident, for flat bottom as well (Fig. 3): The increased intensification is accompanied by a smaller region where the westward propagation can be observed, and it is characterized by a larger westward phase speed, that is, by less inclined isolines in the x–t diagram (compare Fig. 3a with 3b, 7a with 7b, and 8a with 8b).

We have already observed that for topography C no resonant peak appears in the spectum of the response to a white forcing (Fig. 5b, dotted line). This is clearly due to the overwhelming action of the topographic β effect that cancels out any sign of dynamics determined by the planetary β effect. This also implies the absence of westward propagation, as appears evident in Fig. 9, where the continuously forced solution is shown for a forcing frequency Ω chosen equal to the resonant frequency of topography B (any other choice of Ω would lead to analogous conclusions). In this extreme topographic case (corresponding, however, to a typical situation for some Mediterranean subbasins), the response to a monochromatic wind is shaped by the topography and by the spatial variation of the wind stress curl (which in this case is absent being chosen constant over the basin), and no planetary effects intervene to enrich the oceanic dynamics, as it is—on the contrary—the case when less extensive topographies allow for the existence of PRMs. In Fig. 10 it is clearly shown how the fluctuating sea surface elevation (i.e., with a high degree of accuracy, the barotropic streamfunction) reflects closely the isobaths in the case of topography C, while for topographies A and B this happens only over the coastal region where the effect of the topographic gradient is overwhelming, while in the interior the PRM is present. For topographies A and B, one can also notice shelf-trapped oscillations propagating along the shelf that can be interpreted as shelf waves excited either by direct forcing of the wind or by topographic coupling

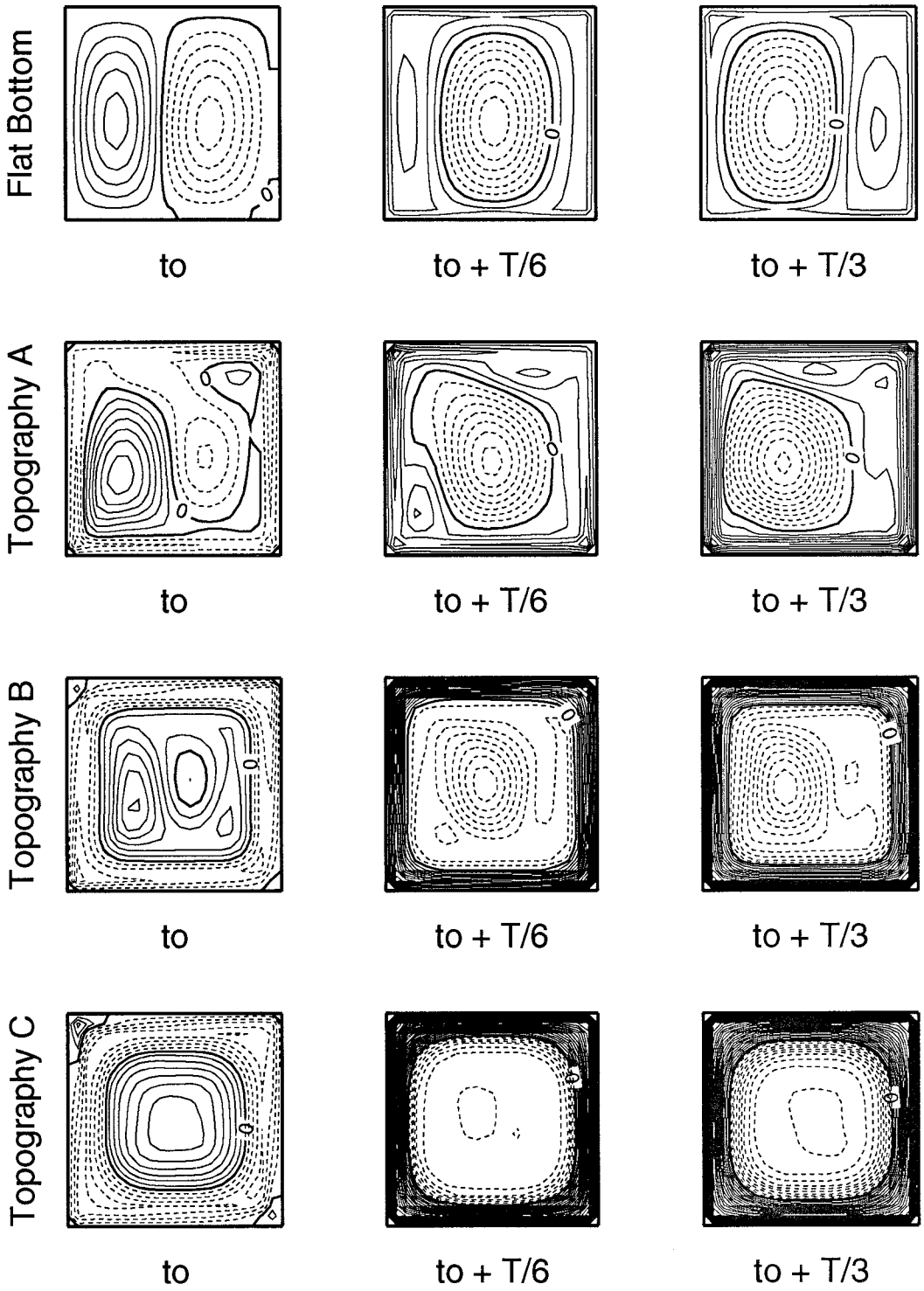

FIG. 10. Snapshots of the sea surface elevation representing a significant part of the whole cycle in the flat-bottom case and for the three topographies considered in this note. The four series of pictures correspond to Fig. 3a (t_0 = 175 d, T = 37.88 d), 7a (t_0 = 165 d, T = 45.45 d), 8a (t_0 = 165 d, T = 62.5 d), and 9a (t_0 = 165 d, T = 62.5 d), respectively.

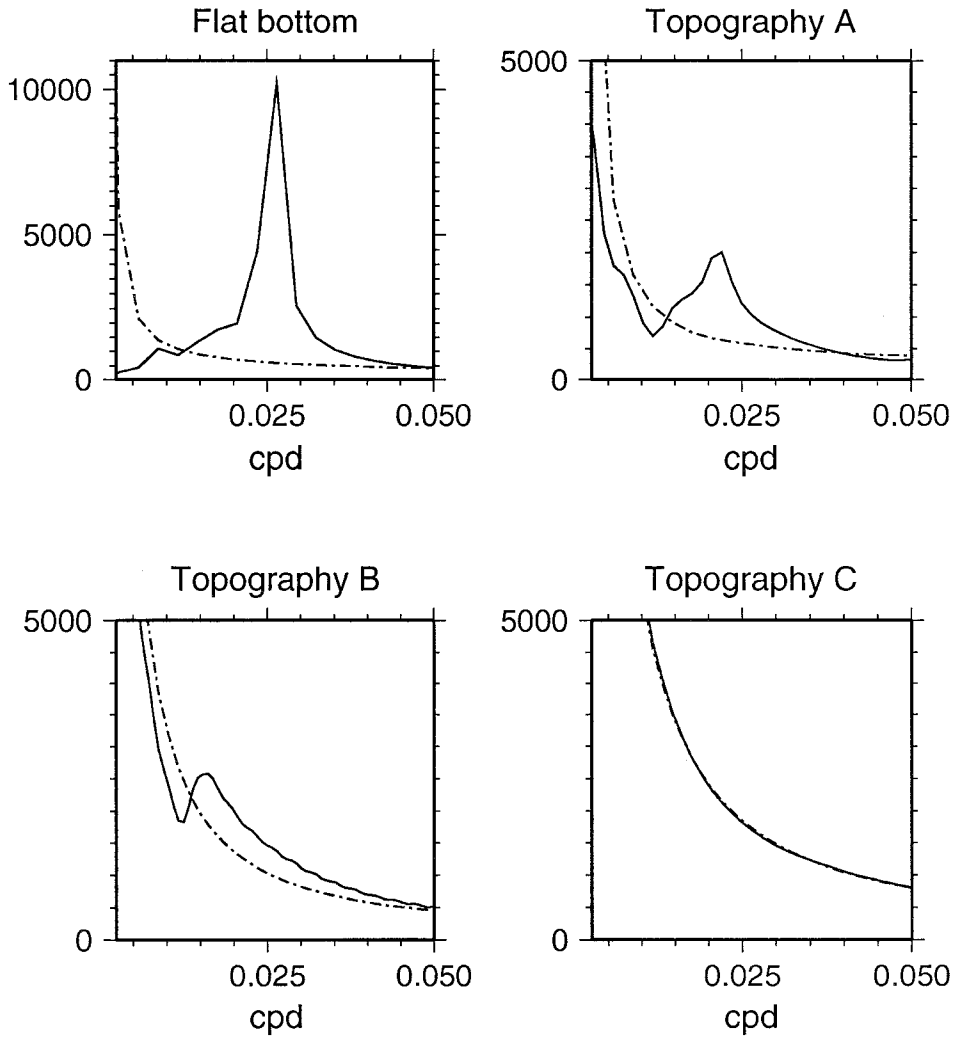

FIG. 11. Numerical solution of (7) forced by (8). Spectra of the sea surface elevation in the middle of the basin (solid lines, see Fig. 5b) and corresponding response for $\beta = 0$ (dashed lines).

with the PRM, as described by Miller (1986) in his study on free PRMs in a similar geometric context.

Figure 11 summarizes in a simple way the results of this section: The solid lines represent the spectra of the responses for the various topographic cases to the white wind forcing (from Fig. 5b), while the dashed lines represent the corresponding spectra obtained by solving the same problem after having removed the planetary β effect, and therefore the Rossby wave dynamics. In the flat-bottom case the two responses do not share any similarity, while for topographies A and B the *f*-plane dynamics suppresses the resonant peak, but the amplitude response is not so divergent from the realistic case away from resonance. For topography C, on the other hand, the two responses are virtually identical, the β effect being totally negligible in this case.

We have therefore some new elements to assess the role played by the planetary β effect in the Mediterranean Sea. It should be noticed that such effect is twofold: (i) it serves as a correction to f_0 in providing a more correct rotation rate at different latitudes and (ii) it provides the restoring force for planetary Rossby waves and modes. As far as point (i) is concerned, Malanotte-Rizzoli and Bergamasco (1989) noticed that the planetary β effect in the Eastern Mediterranean is almost one order of magnitude smaller than the topographic β effect, with the consequence of a virtually identical response to climatological winds with and without β [in a peculiar small-scale region of the Mediterranean such as the Strait of Sicily, Pierini (1996) found that the topographic β effect is more than two orders of magnitude larger than the planetary one, with the consequent possible excitation of localized high-frequency topographic Rossby modes]. Pierini and Simioli (1997) observed that the beta plane is, nevertheless, a better choice than the *f* plane for Mediterranean general circulation studies since, despite the small meridional extension, the βy correction to f_0 is not completely neg-

ligible. As far as point (ii) is concerned, the present results show how the topographic β effect overcomes the planetary one in situations representing extreme idealizations of Mediterranean subbasins. The restoring force provided by the topographic steering for a bottom topography like that of case C (representing very schematically basins such as the Tyrrhenian or the central Ionian Sea) prevents the existence of PRMs. On the other hand, regions of very small topographic gradients are present in the Mediterranean Sea (e.g., the Provençal Basin west of Sardinia or the southwestern Ionian Sea) that resemble more topographies A and B and where therefore the existence of planetary resonances, though modified by the topography as described in this section, cannot in principle be ruled out.

Another obvious consequence of the results of this section is that, if, for instance, for a real topography given by case C one introduces in a circulation model a rough representation of it, say topography B, then the result is the appearence of a spurious resonance (as in the dashed line of Fig. 5b) that is actually absent in the real case (dotted line of Fig. 5b). In other words, the choice of the Mediterranean topography in circulation models should not contain regions of unrealistic flat bottom, otherwise spurious Rossby resonances could contaminate the model response.

In conclusion, the idealized process study presented in this note puts in evidence, in one of the simplest possible ways, the transition from a planetary-controlled dynamics driven by fluctuating winds in a closed domain to a topographically controlled one. Naturally, a single layer model tends to overestimate the effect of bottom topography on the circulation, since the real topographic vortex stretching depends on the bottom velocity instead of the usually larger vertically averaged velocity considered here. Nevertheless, the results presented in this note are expected to describe sufficiently well the role of topography on the wind-driven planetary modes. Finally, although this study originated from the interest in investigating on the possible existence of barotropic planetary Rossby modes in Mediterranean subbasins, general features of planetary modes (such as their westward intensification and relative anomalous behavior as a function of lateral friction in the forced case, and their dependence in frequency and spatial structure on the bottom topography) are determined that can also find application in different world oceans.

Acknowledgments. This research was funded by the European Union Contract MAS2-CT93-0055 (MERMAIDS-II). The author wishes to thank Arthur J. Miller for valuable comments on the manuscript.

REFERENCES

Anderson, D. L. T., and P. D. Killworth, 1977: Spin-up of a stratified ocean with topography. *Deep-Sea Res.,* **24,** 709–732.

Barnier, B., 1984a: Energy transmission by barotropic Rossby waves across large-scale topography. *J. Phys. Oceanogr.,* **14,** 438–447.

——, 1984b: Influence of a mid-ocean ridge on wind-driven barotropic Rossby waves. *J. Phys. Oceanogr.,* **14,** 1930–1936.

Beckers, J. M., 1991: Application of a 3D model to the Western Mediterranean. *J. Mar. Sys.,* **1,** 315–332.

Candela, J., and C. J. Lozano, 1994: Barotropic response of the western Mediterranean to observed atmospheric pressure forcing. *Seasonal and Interannual Variability of the Western Mediterranean Sea, Coastal Estuarine Studies,* P. La Violette, Ed., Vol. 46, Amer. Geophys. Union, 325–359.

Carton, J. A., 1983: The variation with frequency of the long-period tides. *J. Geophys. Res.,* **88,** 7563–7571.

Frankignoul, C., and P. Müller, 1979: Quasigeostrophic response on an infinite β-plane ocean to stochastic forcing by the atmosphere. *J. Phys. Oceanogr.,* **9,** 104–127.

Harrison, D. E., 1979: On the equilibrium linear basin response to fluctuating winds and mesoscale motions in the ocean. *J. Geophys. Res.,* **84,** 1221–1224.

Heburn, G. W., 1994: The dynamics of the seasonal variability of the Western Mediterranean circulation. *Seasonal and Interannual Variability of the Western Mediterranean Sea, Coastal Estuarine Studies,* P. La Violette, Ed., Vol. 46, Amer. Geophys. Union, 249–285.

Herbaut, C., L. Mortier, and M. Crépon, 1996: A sensitivity study of the general circulation of the Western Mediterranean Sea. Part I: The response to density forcing through the straits. *J. Phys. Oceanogr.,* **26,** 65–84.

Kroll, J., and P. P. Niiler, 1976: The transmission and decay of barotropic Rossby waves incident on a continental shelf. *J. Phys. Oceanogr.,* **6,** 432–450.

Le Blond, P. H., and L. A. Mysak, 1978: *Waves in the Ocean.* Elsevier, 602 pp.

Leetma, A., 1978: Fluctuating winds: An energy source for mesoscale motions. *J. Geophys. Res.,* **83,** 427–430.

Luther, D. S., 1982: Evidence of a 4–6 day barotropic, planetary oscillation of the Pacific Ocean. *J. Phys. Oceanogr.,* **12,** 644–657.

Malanotte-Rizzoli, P., and R. E. Young, 1988: Numerical simulations of transient boundary-forced radiation. Part II: The modon regime. *J. Phys. Oceanogr.,* **18,** 1546–1569.

——, and A. Bergamasco, 1989: The circulation of the Eastern Mediterranean. I. *Oceanol. Acta,* **12,** 335–351.

——, and ——, 1991: The wind and thermally driven circulation of the eastern Mediterranean Sea. Part II: The baroclinic case. *Dyn. Atmos. Oceans,* **15,** 355–371.

——, D. B. Haidvogel, and R. E. Young, 1987: Numerical simulations of transient boundary-forced radiation. Part I: The linear regime. *J. Phys. Oceanogr.,* **17,** 1439–1457.

Matano, R. P., 1995: Numerical experiments on the effects of a meridional ridge on the transmission of energy by barotropic Rossby waves. *J. Geophys. Res.,* **100,** 18 271–18 280.

Miller, A. J., 1986: Nondivergent planetary oscillations in midlatitude ocean basins with continental shelves. *J. Phys. Oceanogr.,* **16,** 1914–1928.

——, W. R. Holland, and M. C. Hendershott, 1987: Open-ocean response and normal mode excitation in an eddy-resolving general circulation model. *Geophys. Astrophys. Fluid Dyn.,* **37,** 253–278.

——, D. S. Luther, and M. C. Hendershott, 1993: The fortnightly and monthly tides: Resonant Rossby waves or nearly equilibrium gravity waves? *J. Phys. Oceanogr.,* **23,** 879–897.

——, P. F. J. Lermusiaux, and P. M. Poulain, 1996: A topographic Rossby mode resonance over the Iceland–Faeroe ridge. *J. Phys. Oceanogr.,* **26,** 2737–2747.

Millot, C., 1987: Circulation in the Western Mediterranean Sea. *Oceanol. Acta,* **10,** 143–149.

Pedlosky, J., 1965a: A note on the western intensification of the oceanic circulation. *J. Mar. Res.,* **23,** 207–209.

——, 1965b: A study of the time dependent ocean circulation. *J. Atmos. Sci.,* **22,** 267–272.

——, 1977: On the radiation of mesoscale energy in the mid-ocean. *Deep-Sea Res.,* **24,** 591–600.
——, 1987: *Geophysical Fluid Dynamics.* Springer-Verlag, 710 pp.
Pierini, S., 1990: A divergent quasi-geostrophic model for wind-driven oceanic fluctuations in a closed basin. *Dyn. Atmos. Oceans,* **14,** 259–277; Corrigendum, **14,** 415.
——, 1996: Topographic Rossby modes in the Strait of Sicily. *J. Geophys. Res.,* **101,** 6429–6440.
——, and A. Simioli, 1997: A wind-driven circulation model of the Tyrrhenian Sea area. *J. Mar. Sys.,* in press.
Pinardi, N., and A. Navarra, 1993: Baroclinic wind adjustment processes in the Mediterranean Sea. *Deep-Sea Res.,* **40,** 1299–1326.
——, G. Korres, A. Lascaratos, V. Roussenov, and E. Stanev, 1997: Numerical simulation of the interannual variability of the Mediterranean Sea upper ocean circulation. *Geophys. Res. Lett.,* in press.
Rhines, P. B., 1969: Slow oscillations in an ocean of varying depth. Part 1. Abrupt topography. *J. Fluid Mech.,* **37,** 161–189.
Robinson, A. R., M. Colnaraghi, W. G. Leslie, A. Artegiani, A. Hecht, E. Lazzoni, A. Michelato, E. Sansone, A. Theocharis, and U. Unlüata, 1991: Structure and variability of the Eastern Mediterranean general circulation. *Dyn. Atmos. Oceans,* **15,** 215–240.
Roussenov, V., E. Stanev, V. Artale, and N. Pinardi, 1995: A seasonal model of the Mediterranean Sea general circulation. *J. Geophys. Res.,* **100,** 13 515–13 538.
Wang, L., and C. J. Koblinsky, 1994: Influence of mid-ocean ridges on Rossby waves. *J. Geophys. Res.,* **99,** 25 143–25 153.
Willebrand, J., S. G. H. Philander, and R. C. Pacanowski, 1980: The oceanic response to large-scale atmospheric disturbances. *J. Phys. Oceanogr.,* **10,** 411–429.
Wunsch, C., 1967: The long-period tides. *Rev. Geophys.,* **5,** 447–475.
Zavatarelli, M., and G. L. Mellor, 1995: A numerical study of the Mediterranean Sea circulation. *J. Phys. Oceanogr.,* **25,** 1384–1414.